Haploinsufficiency of Insm1 impairs postnatal baseline beta-cell mass

Tao S, Zhang Y, Ma L, Deng C, Duan H, Liang X, Liao R, Lin S, Nie T, Chen W, Wang C, Birchmeier C, Jia S

Diabetes
2018 NOV 20 ; 67(12): 2615-2625
2018 SEP 26 (first published online)
doi: 10.2337/db17-1330

Publisher: American Diabetes Association

Haploinsufficiency of Insm1 impairs postnatal baseline beta-cell mass

Weihua Tao[1#], Yao Zhang[2#], Lijuan Ma[1], Chujun Deng[1], Hualin Duan[1], Xuehua Liang[1], Rui Liao[1], Shaoqiang Lin[1], Tao Nie[1,4], Wanqun Chen[3], Cunchuan Wang[1], Carmen Birchmeier[2], Shiqi Jia[* 1,2,4]

[1] The First Affiliated Hospital of Jinan University, Guangzhou, China

[2] Developmental Biology/Signal Transduction Group, Max-Delbrück-Center for Molecular Medicine, Berlin, Germany

[3] Department of Biochemistry and Molecular Biology, School of Basic Medical Science, Jinan University, Guangzhou, China

[4] Institute of Clinical Medicine, Jinan University, Guangzhou, China

#These authors contributed equally to this work

* Corresponding authors:

Shiqi Jia, Phone: +86-20-3868 0563, Email: jshiqi@aliyun.com

Abstract

Baseline beta-cell mass is established during the early postnatal period when beta cells expand. Here, we show that heterozygous ablation of *Insm1* decreases baseline beta-cell mass and subsequently impairs glucose tolerance. When exposed to a high-fat diet or on an *ob/ob* background, glucose intolerance was more severe in *Insm1*$^{+/lacZ}$ mice compared to *Insm1*$^{+/+}$ mice, although no further decrease in the beta-cell mass was detected. In islets of early postnatal *Insm1*$^{+/lacZ}$ mice, cell cycle was prolonged in beta cells due to downregulation of the cell cycle gene *Ccnd1*. Although Insm1 had a low affinity for the *Ccnd1* promoter compared to other binding sites, binding affinity was strongly dependent on Insm1 levels. We observed dramatically decreased binding of Insm1 to the *Ccnd1* promoter after downregulation of *Insm1* expression. Furthermore, downregulation of *Ccnd1* resulted in a prolonged cell cycle and overexpression of Ccnd1 rescued cell cycle abnormalities observed in Insm1-deficient beta cells. We conclude that decreases in Insm1 interfere with beta-cell specification during the early postnatal period and impair glucose homeostasis during metabolic stress in adults. Insm1 levels are therefore a factor that can influence the development of diabetes.

Introduction

Pancreatic beta-cell mass is regulated both during development and in the adult. Lineage tracing in animals indicates that embryonic beta cells mainly differentiate from pancreatic progenitor cells [1], while postnatal increases in beta-cell mass arise through self-renewal [2, 3]. Beta-cell replication slows

considerably in adults, although variations in insulin demand can lead to adaptive changes in beta-cell mass [4]. Sufficient beta-cell mass is essential for normal regulation of blood glucose levels. Loss of beta-cell mass by an immune attack or metabolic stressors results in type 1 and type 2 diabetes, respectively. In addition, although beta-cell mass varies in individuals, low beta-cell mass is a risk factor for prediabetes and diabetes [5]. At least two factors contribute to total beta-cell mass: replication capacity and baseline beta-cell mass. The replication rate of adult beta cells is low, and massive efforts have been made to restore diabetic beta-cell loss by enhancing beta-cell replication. In contrast, the establishment of the baseline beta-cell mass is not well investigated, and it is not yet fully understood how postnatal beta-cell expansion varies in different individuals.

The baseline beta-cell mass is established in the early postnatal period both in mice and humans [2, 6-8]. Recent identified factors that modulate the postnatal beta-cell expansion regulate the metabolic pathways or the cell cycle [9, 10, 11]. The cyclin genes *Ccnd1* and *Ccnd2* are essential for postnatal beta-cell growth and regulate the progression through G1 through interaction with Cdk4 [12-14]. Heterozygous mutations in *Ccnd1* combined with complete knockout of *Ccnd2* has dose-dependent effects on beta-cell mass [14]. Cell cycle inhibitors are another group of essential regulators in the postnatal beta-cell mass expansion. $p16^{INK4a}$ is a beta-cell replication inhibitor specifically expressed in aging beta cells. Therefore, although mutation of $p16^{INK4a}$ has no effect on the early postnatal beta-cell mass, overexpression of $p16^{INK4a}$ decreases postnatal beta-cell mass [15]. p21, p27 and p57 regulate

the cell cycle in embryonic beta cells [16, 17] as well as postnatal pancreatic beta-cell proliferation [18].

Insm1 encodes a zinc finger protein that is essential for the development and function of mature beta cells. Null mutation of *Insm1* interferes with the formation of insulin positive beta cells [19, 20], whereas deletion of *Insm1* in adult beta cells leads to loss of mature beta-cell function [21]. Here, we show that Insm1 haploinsufficiency impairs the early postnatal beta-cell expansion, resulting in decreased baseline beta-cell mass and impaired glucose tolerance. Mechanistically, the decreased dosage of Insm1 prolongs the cell cycle in part by targeting *Ccnd1*. Insm1 binds to the *Ccnd1* locus with low affinity in beta cells and binding is dramatically lost upon downregulation of *Insm1*. Our data demonstrate that Insm1 regulates postnatal baseline beta-cell mass in a dose-dependent manner, indicating that decreased Insm1 expression is a potential risk factor for diabetes.

Research Design and Methods

Animals and genotyping

The *Insm1*^{lacZ} allele was reported previously [19]. Male animals were used for all experiments. Wild-type littermates were used as controls. A high-fat diet treatment was started at 3 months of age, and glucose tolerance and the beta-cell mass was measured after 10-months on the high-fat diet. *Ob/ob* mice were analyzed at 13 months of age. All animal experiments were approved by the Institutional Animal Care and Use Committee of Jinan University.

Blood glucose levels, insulin levels and beta-cell mass

Blood glucose and blood insulin measurements were performed as previously described [21]. Briefly, blood glucose levels from each animal were determined from at least three independent measurements on different days. Blood insulin levels from each animal were determined from average values obtained from at least two independent measurements on different days. For glucose tolerance and insulin secretion tests, glucose was injected intraperitoneally (2 g/kg body weight, unless otherwise indicated). Insulin and glucagon ELISA kits were used to detect insulin and glucagon levels in the blood (90080, Crystal Chem, Downers Grove, USA; DGCG0, Quantikine® ELISA, R&D Systems, Inc., MN, USA)

Beta-cell mass was determined as previously described [21]. In short, each pancreas was evenly flattened and fixed in 4% PFA for 3 hours, embedded in paraffin, and then sectioned at 8 μm thickness. For beta-cell mass analysis, we collected sections every 10th sections in 2-, 7- and 14-day old animals, and every 20th sections in 2-month, 13-month, HFD and ob mice; that is, approximately 8-10 pancreatic sections for each animal were used. Beta-cell area was identified by immunofluorescence using anti-insulin antibodies. The total area of the pancreas, insulin-positive area and pancreas weight were used to calculate beta-cell mass: beta-cell mass (mg/pancreas) = whole pancreas weight (mg) * insulin positive area/pancreas area. Image J software was used to quantify the areas of pancreas and beta-cell.

Immunofluorescence and Western blot

Immunofluorescence and Western blots were performed as described [21]. Fluorescence was imaged on a Zeiss LSM 700 confocal microscopy and processed using Adobe Photoshop software. Anti-Insm1, anti-insulin, anti-

Glut2, anti-BrdU and anti-ActB antibodies were used as previously described [21], and anti-Ccnd1 antibody was purchased from Abcam (ab-134175) and Santa Cruz (sc-753). Anti-Ki67 antibody was purchased from Dako (M7249) and Abcam (ab15580). Anti-p16 (ab51243, Abcam), anti-p21 (ab109199, Abcam), anti-p27 (ab92741, Abcam), anti-p57 (ab75974, Abcam), anti-CcnE1 (20808S, CST) and anti-CcnA2 (ab181591, Abcam) antibodies were used for Western blotting. Secondary antibodies (Jackson ImmunoResearch) coupled to Cy3, Cy2, Cy5 (for immunofluorescence) or horseradish peroxidase (for Western blot) were used.

Pancreatic islets isolation and insulin secretion assay

Pancreatic islets were isolated as previously described [21]. The assay was performed by incubating islets for 30 min in secretion buffer containing 3.3 mM or 16.7 mM glucose with washing and pre-incubation steps between and before the assay [21]. Released insulin was quantified using an ELISA kit (80-INSMSH, ALPCO, NH, USA) as described [21].

qRT-PCR analysis

Freshly isolated islets or cultured SJb cells were lysed, and total RNA was isolated using Trizol reagent (Invitrogen). For qRT-PCR analysis, cDNA from each animal was synthetized using PrimeScript™ RT reagent Kit with gDNA Eraser (TakaRa, China) and analyzed using SYBR® Fast qPCR Mix (TaKaRa, China) on CFX96 RT-PCR system (Bio-Rad). Expression levels were determined using the $2^{-\Delta\Delta Ct}$ method. *ActB* was used as internal standard, and the results were displayed as the proportion of wild-type controls. Primers used for quantitative analysis are listed in Supplemental Table S1.

ChIP-PCR

For ChIP-PCR, we used isolated pancreatic islets or SJb beta-cell line. Anti-Insm1 antibody was used for ChIP-PCR as described in our previous study [21]. The PCR primers used for chromatin analysis are shown in Supplemental Table S1.

siRNA knockdown

siRNAs against *Insm1* and *Ccnd1* mRNAs were delivered by electroporation with the Amaxa Nucleofector using the Amaxa kit V and program G-16, according to the protocols provided by the kits. Mouse *Insm1* and nontargeting control siRNAs were purchased from Dharmacon (J-049233 -09/-11/-12 for *Insm1* and D-001810-10 for control). Mouse *Ccnd1* siRNAs were purchased from Ambion (s63513, s201129).

PI staining and flow cytometer analysis

Alcohol fixed SJb cells were washed with PBS and incubated with PBS containing 0.1% Triton-X-100, 3 mg/mL DNase-free RNase (EN0531, Thermo Fisher) and 20 µg/µL propidium iodide (Biofroxx, Germany) for 15 min at 37°C. Cells were directly analyzed on an LSR Fortessa analyzer (Beckton Dickenson, Franklin Lakes, USA). Cell cycle distributions were calculated using the Dean-Jett model in FloJo X10.0.7r2. A representative result from 4 biological independent experiments was shown.

Results

Impaired glucose tolerance and beta-cell mass in *Insm1* heterozygote mice

To investigate the effects of *Insm1* gene dosage on beta-cell function, we used *Insm1*$^{+/lacZ}$ mice that harbor one intact *Insm1* allele and one mutant allele in which *lacZ* replaces the *Insm1* coding sequence [19]. In *Insm1*$^{+/lacZ}$ islets, Insm1 protein levels were lower at 2-months or 2-weeks of age (Fig. 1A, Fig. S1). Compared to *Insm1*$^{+/+}$ mice, blood glucose levels were significantly higher in *Insm1*$^{+/lacZ}$ mice on a random feeding schedule, while the fasting blood glucose levels were comparable (Fig. 1B). *Insm1*$^{+/lacZ}$ mice were glucose intolerant (Fig. 1C) and displayed defects in glucose stimulated insulin secretion (Fig. 1D). Although the blood glucagon levels were comparable in *Insm1*$^{+/lacZ}$ and *Insm1*$^{+/+}$ mice in both fasted and randomly fed conditions (Fig. 1E), the proportions of glucagon-producing alpha cells and other endocrine cell types were not altered (Fig. S2). Moreover, there was no change in peripheral insulin sensitivity in *Insm1*$^{+/lacZ}$ mice using an insulin tolerance test (Fig. 1F). We isolated islets and performed glucose-stimulated insulin secretion ex vivo. We observed comparable levels of insulin secretion in islets from both genotypes at low and high glucose concentrations (Fig. 1G). In *Insm1*$^{+/lacZ}$ mice, we observed reduced insulin secretion in vivo but normal secretion in isolated islets, indicating insufficient beta-cell mass. Indeed, we observed that the beta-cell mass in *Insm1*$^{+/lacZ}$ mice was 70.9% of that of *Insm1*$^{+/+}$ mice at 2-months (P2 M) (Fig. 1H). This decrease in beta-cell mass was not caused by differences in beta-cell size, as comparable cell sizes were observed in wide-type and *Insm1*$^{+/lacZ}$ mice (Fig. S3).

To further dissect the time course of the deficits, we measured beta-cell mass in postnatal 2-day (P2), 7-day (P7), 14-day (P14) and 13-month (P13M) (Fig. 1H). We observed comparable beta-cell mass between newborn (P2)

Insm1$^{+/+}$ and *Insm1*$^{+/lacZ}$ mice. A small, but not significant, decrease in beta-cell mass was detected at P7 in *Insm1*$^{+/lacZ}$ mice. Significant decreases in beta-cell mass were detected at P14, when the beta-cell mass of *Insm1*$^{+/lacZ}$ mice was 77.6% of that observed in *Insm1*$^{+/+}$ mice. A further decrease in beta-cell mass was detected at P2M in *Insm1*$^{+/lacZ}$ mice (70.9% at P2M vs P77.6% at P14, p=0.0058). However, there were no further differences in beta-cell mass between *Insm1*$^{+/lacZ}$ and *Insm1*$^{+/+}$ mice after P2M, as beta-cell mass remained approximately 70.9% at P2M and 65.9% at P13M (p=0.7798) (Fig. 1H). These data indicated that the impaired beta-cell expansion occurs in the postnatal period between 7-days and 2-months.

Delayed cell cycle in beta-cell of *Insm1* heterozygotes mice

Because we first observed significant changes in beta-cell mass at P14, we used this time point to analyze in vivo experiments, unless otherwise indicated. Increased TUNEL staining in *Insm1*$^{+/lacZ}$ beta cells were detected at both P7 and P14 but not at P2 (Fig. 2A), while proliferation, indicated by the presence of Ki67, was comparable (Fig. 2B). Thus, increased apoptosis contributes to the low beta-cell mass in *Insm1*$^{+/lacZ}$ mice. However, we noticed that the apoptosis rate was much lower than the rate of proliferation (i.e., 1.5 apoptotic cells per 1000 insulin positive cells versus 180 proliferated cells per 1000 insulin positive cells at P7) (Fig. 2A, B), suggesting that apoptosis might not be a major contributor to the decrease in beta-cell mass.

We investigated cell cycle length using BrdU pulse-chase combined with Ki67 staining in P14 *Insm1*$^{+/lacZ}$ and *Insm1*$^{+/+}$ mice. A single pulse of BrdU was administered to mice followed by a 23-hour chase period, the approximate

amount of time needed to complete one cycle of cell division [22]. BrdU labeling was retained by the cells within the cell cycle as well as those that had reached a postmitotic state, while Ki67 only labeled the cells in the cell cycle. Thus, $BrdU^{+}Ki67^{-}$ cells had exited the cell cycle while $BrdU^{+}Ki67^{+}$ cells had not yet completed the cell cycle (Fig. 2C). We found significantly decreased numbers of $BrdU^{+}Ki67^{-}$ cells and increased numbers of $BrdU^{+}Ki67^{+}$ cells in *Insm1*$^{+/lacZ}$ mice (Fig. 2D, E), indicating that cell cycle length in *Insm1*$^{+/lacZ}$ beta cells was prolonged. This prolonged cell cycle could be repeatedly detected at 3 weeks but not at 10 weeks in *Insm1*$^{+/lacZ}$ mice (Fig. S4A). We further counted cell numbers in different phases of the cell cycle using propidium iodide (PI) staining and flow cytometry analysis. Knockdown of Insm1 in SJb cells, a previously described pancreatic beta-cell line that retains many of the in vivo characteristics of beta cells [21], resulted in a small, but significant increase, in cells in G0/G1 (Fig. 3A). Thus, haploinsufficiency of Insm1 in beta cells delays the cell cycle.

Because we observed delayed cell cycle and increased apoptosis in *Insm1*$^{+/lacZ}$ mice, we asked whether abnormalities in cell cycle caused cell death. We performed TUNEL staining followed by immunofluorescence analysis using Ki67 staining. However, we did not detect any costaining of TUNEL and Ki67 in over 1000 Ki67+ cells per animal at postnatal day 14 (data not shown). Although decreases in Insm1 led to a longer cell cycle, proliferating cells did not directly enter cell death in *Insm1*$^{+/lacZ}$ islets.

Ccnd1 expression levels are downregulated in islets of _Insm1_ heterozygotes mice

The cell cycle is marked and regulated by numerous cyclin genes [23, 24]. We investigated the expression of cyclin, cyclin kinase and cyclin kinase inhibitor genes. We found that of the G1/S phase cyclins, only *Ccnd1* was downregulated in P14 *Insm1*$^{+/lacZ}$ islets (Fig. 3B). *Ccnd1* was further downregulated in SJb cells treated with *Insm1* siRNA and in P7 *Insm1*$^{+/lacZ}$ islets (Fig. S4B, C). We further verified decreases in Ccnd1 protein but not other cell cycle regulators in islets isolated from P14 *Insm1*$^{+/lacZ}$ mice (Fig. 3C and Fig. S5A). Because *Ccnd1* expression was consistently decreased in both early and postnatal *Insm1*$^{+/lacZ}$ islets and *Insm1* deficient SJb cells, we investigated the regulation of cell cycle length by Ccnd1.

Knockdown of *Insm1* by siRNA in SJb cells resulted in fewer BrdU^{+}Ki67^{-} cells and an increase in BrdU^{+}Ki67^{+} cells (Fig. 3D). Similar changes were observed after knockdown of *Ccnd1* expression (Fig. 3D). Next, we overexpressed *Ccnd1* in SJb cells treated with *Insm1* siRNA. Significantly increased numbers of BrdU^{+}Ki67^{-} cells and decreased numbers of Brdu^{+}Ki67^{+} cells were observed, demonstrating that the downregulation of *Insm1* expression can be rescued by overexpressing *Ccnd1* (Fig. 3D). PI labeling and flow cytometry cell cycle analysis showed that significant increases in cell number were detected in the G0/G1 phase in *Insm1* or *Ccnd1* knockdown cells, while overexpression of *Ccnd1* in *Insm1* knockdown SJb cells rescued the increasing of G0/G1 phase cell numbers (Fig. 3A). In summary, *Ccnd1* is a downstream target of Insm1 and controls cell cycle length.

In our previous study, we observed downregulation of many metabolic genes and transcription factors in islets after conditional ablation of *Insm1* [21], leading us to investigate the expression of these genes in *Insm1*$^{+/lacZ}$ islets.

We detected downregulation of *Glut2* but no change in *Pcx, Hk1, Pdx1* or *MafA* (Fig. 4A,B, Fig. 5SB), suggesting that Insm1 target gene *Glut2* is regulated in a dose-dependent manner by Insm1.

Binding of Insm1 on low affinity targets depends on Insm1 dose

To investigate the mechanisms of Insm1-dependent regulation of *Ccnd1*, we analyzed Insm1 ChIP-seq data [21]. We observed binding of Insm1 on both the promoter and intron regions of *Ccnd1* (Fig. 5A). The number of reads on the *Ccnd1* gene observed in the ChIP-seq data set was lower than that detected in other Insm1 binding genes, such as the *Pdx1* and *Hk1* genes. However, Insm1 broadly binds to *Pdx1*, and these binding sites belong to a cluster of enhancers called superenhancers [25, 26], which is therefore high-affinity binding (Fig. 5A). To determine how levels of Insm1 influenced binding to chromatin, we performed ChIP-PCR on control and *Insm1* siRNA-treated SJb cells. Knockdown of *Insm1* reduced Insm1 protein levels (Fig. 5B, left), and binding of Insm1 on *Hk1, Pdx1* and *Glut2* decreased by 1.4-, 1.7- and 5.7-fold, respectively. The decrease of Insm1 binding to the promoter and intron regions of *Ccnd1* was more pronounced, where an 8.8- and 10.3-fold decrease, respectively, was observed after *Insm1* knockdown (Fig. 5B right). We further verified the decreased binding of Insm1 on the *Ccnd1* and *Glut2* loci in P14 $Insm1^{+/lacZ}$ islets (Fig. 5C). These data indicated that the low affinity binding sites were prone to losing Insm1 binding in response to decreases in Insm1. In summary, Insm1 binds to *Ccnd1* and *Glut2* with relatively low affinity, and this binding is sensitive to changes in levels of Insm1.

Metabolic stress aggravates glucose intolerance in *Insm1* heterozygotes mice

To investigate the effect of Insm1 haploinsufficiency on the glycemic phenotype after metabolic stress, we introduced the *Insm1*$^{+/lacZ}$ allele into the *ob/ob* background. We performed glucose tolerance tests (glucose was administered at 0.5 g/kg body weight) and observed severe glucose intolerance (Fig. 6A). The glucose tolerance of *Insm1*$^{+/lacZ}$ mice in the *ob/ob* background was much lower than observed in age matched wild-type animals (Fig. 6B). Similarly, *Insm1*$^{+/lacZ}$ mice on a high-fat diet (HFD) showed further decreases in glucose tolerance (Fig. 6C). Although the fasted blood glucose levels in *Insm1*$^{+/lacZ}$ mice were comparable to *Insm1*$^{+/+}$ mice on an HFD, these levels increased in an *ob/ob* background (Fig. 6D). Random blood glucose levels were consistently higher in *Insm1*$^{+/lacZ}$ mice either on an HFD or in an *ob/ob* background (Fig. 6E).

To investigate whether the beta-cell mass of *Insm1*$^{+/lacZ}$ mice is further decreased during metabolic stress, we measured the beta-cell mass after HFD treatment or in an *ob/ob* background. In *Insm1*$^{+/+}$ animals, beta-cell mass increased to 7.96 mg and 11.92 mg, while the mass in *Insm1*$^{+/lacZ}$ mice was 5.22 mg and 7.56 mg in HFD treated or *ob/ob* background animals, respectively (Fig. 6F). The ratio of beta-cell mass (*Insm1*$^{+/lacZ}$ vs *Insm1*$^{+/+}$) was similar in animals on a high-fat diet (65.6%) or in an *ob/ob* background (63.5%) compared to age matched animals on a normal diet (65.9%; unpaired t-test, p=0.94 for HFD and p=0.84 for *ob/ob*). We investigated the expression of *Ccnd1* and *Glut2* in islets of 13-month-old mice and found comparable expression of *Ccnd1* but decreased *Glut2* expression in *Insm1*$^{+/lacZ}$ compared

to *Insm1*$^{+/+}$ mice (Fig. 6G). We performed ChIP-PCR in the aging islets; we found comparable Insm1 binding to the *Ccnd1* locus but lower binding to the *Glut2* locus in *Insm1*$^{+/lacZ}$ mice (Fig. 6H). Together, our data indicate that the Insm1 dosage is particularly important for *Ccnd1* expression and the establishment of beta-cell mass specifically at early postnatal stages. Thus, decreases in beta-cell mass and *Glut2* expression in *Insm1*$^{+/lacZ}$ animals contribute to impaired glucose handling during metabolic stress.

Discussion

Ccnd1 gene is regulated at the transcriptional and translational levels [27, 28, 29]. We found that *Ccnd1* transcription is dependent on Insm1 dosage and the protein level is also decreased in beta cells *of Insm*$^{+/lacZ}$ mice. Thus, Insm1 can transcriptionally regulate the cell cycle by targeting *Ccnd1*. Our previous work elucidated that the protein complex Insm1/NeuroD1/FoxA2 binds with high affinity to pancreatic beta-cell genes that play an essential role in maintaining mature beta-cell function [21]. Here, we identified that Insm1 dosage mainly affects the low affinity binding sites, i.e., the *Ccnd1* locus. Thus, we elucidated a novel mechanism of Insm1 function in pancreatic beta cells.

We show here that the decreased baseline beta-cell mass established at early postnatal stages in the *Insm1*$^{+/lacZ}$ mice was unchanged in the adult with or without metabolic stress. Thus, at least in the *Insm1*$^{+/lacZ}$ mice, the baseline beta-cell mass established in the early postnatal period determined the functional beta cells in the adult; it will be interesting to see whether this is a

general phenomenon. In addition, we observed that *Ccnd1* expression was not downregulated in the islets of the adult *Insm1*$^{+/lacZ}$ mice. This suggests that Insm1 might not be involved in regulating *Ccnd1* expression in adult beta cells, or that one allele of *Insm1* is sufficient to support the very low proliferation rate and *Ccnd1* expression in adult beta cells. We did not observe decreases in beta-cell mass in the newborn *Insm1*$^{+/lacZ}$ mice, indicating that Insm1 dosage has little effect on beta-cell development. Prenatal beta cells differentiate from stem/progenitor cells [1], while the postnatal beta-cell expansion arises from the self-duplication of beta cells [3]. There are different scenarios to describe regulation of beta-cell mass in the two different developmental stages. For instance, *Nkx6.1* is required for postnatal, but not prenatal, beta-cell mass expansion [9]; *Ccnd1*, identified as a target of Insm1 in our work, does not contribute to prenatal beta-cell growth [13, 14]. We found that Insm1 dosage regulates *Glut2* expression. *Glut2*, an gene essential for glucose sensing and metabolism, was markedly reduced in diabetic animals [30, 31, 32]. We observed a decrease of approximately 40% in Glut2 expression in the islets of *Insm1*$^{+/lacZ}$ mice, which could contribute to the impaired glucose handling under physiological or metabolically stressed conditions.

We showed that changes in Insm1 expression only regulate a few Insm1 targets, which were identified in *Insm1* null mutation (as showed in Fig. 3B and Fig. 4A). The cell cycle genes *Cdkn1c (p57), Cdkn1b (p27)* and *Ccnd1* were downregulated in *Insm1* null mutants [20, 21], but only *Ccnd1* was downregulated in *Insm1* heterozygotes (Fig. 3B). The transcription factors and

metabolic genes *Pdx1, MafA, Glut2, Hk1* and *Pcx* were downregulated in *Insm1* mutants [21]. However, only *Glut2* was downregulated in *Insm1* heterozygotes (Fig. 4A). We found that the binding affinity of Insm1 to chromatin varied depending on the locus. Low affinity binding sites were more susceptible to decreases in Insm1 levels and therefore to be potentially affected by Insm1 dosage deficiency. Loci with no affinity or high affinity for did not show dysregulation of the related genes in *Insm1*$^{+/lacZ}$ islets (Fig. S5C and Fig. 3B; Fig. 5A and Fig. 4A). Thus, only genes that have relatively low Insm1 binding affinity are potentially regulated by Insm1 in a dose-dependent manner.

Osipovich *et al.* observed increased *Ccnd1* expression and 7-fold decreased proliferation in embryonic pancreatic beta cells in the absence of *Insm1* [20], as well as a slight increase in proliferation and decrease in *Ccnd1* expression in mature *Insm1* deficient beta cells [21]. These studies investigated Insm1 function at embryonic or adult stages in the absence of *Insm1* and did not study dose-dependent effects. Embryonic loss of *Insm1* results in severe developmental defects (loss of beta-cell development and no insulin production [19, 33]), and conditional loss of *Insm1* in adult islets causes functional defects (continuous leak of insulin). However, *Ccnd1* expression is not only directly regulated by Insm1 but also indirectly regulated by these defects. In fact, insulin and glucose are essential regulators of beta-cell proliferation [34,35]. Severe developmental defects, abnormal blood insulin and glucose levels, or higher numbers of and/or more intense dysregulated genes other than *Ccnd1* all contribute to the proliferation defects observed in

complete or conditional mutants of *Insm1*. In our present study, we used *Insm1*$^{+/lacZ}$ mice, which have mild defects in blood glucose and insulin levels. We found that Insm1 regulates *Ccnd1* expression and cell cycle length in a dose dependent manner.

Zhang and Lan showed that the Insm1 protein can interact with Ccnd1 and Ckd4 [36]. Ectopic expression of Insm1 interrupts Ccnd1-Cdk4 function and negatively regulates the cell cycle [36, 37]. In Zhang and Lan's work, they defined Insm1 function in nonpancreatic beta cells. Interestingly, abnormally high Insm1 expression levels were observed in neuroendocrine tumors, including insulinoma cells, which are highly proliferative [38-45]. Tissue specific factors can play distinct roles in cell cycle control in different cell types, and one dramatic example is provided by the transcription factor RE1 silencing transcription factor (REST) [46]. Additional investigation is required to determine whether Insm1 performs similar or different functions in regulating the Ccnd1-Cdk4 complex and cell cycle in pancreatic beta cells using additional Insm1 mutant models.

We detected increased apoptosis in pancreatic beta cells from *Insm1*$^{+/lacZ}$ mice. *Neurod1* and *Pdx1* regulate beta-cell apoptosis in prenatal or aging mice [47,48]. Insm1 can bind the *Neurod1* promoter and can also regulate the expression of *Pdx1* [49, 21]. However, our current study showed that Insm1 dosage does not regulate the expression of these genes, illustrating a difference between haploinsufficiency and complete loss of function mutations. Furthermore, we did not find an association between delayed cell

cycle and apoptosis in *Insm1*$^{+/lacZ}$ beta cells. Thus, the increase in apoptosis in beta cells of *Insm1*$^{+/lacZ}$ mice is likely independent of the observed cell cycle delay and requires further investigation.

Acknowledgments. The authors thank Bettina Brandt (Max Delbrück Center for Molecular Medicine) for technical assistance and Claudia Paeseler (Max Delbrück Center for Molecular Medicine) for animal husbandry. The authors thank Dr. Michael Strehle (Max Delbrück Center for Molecular Medicine) for editing the language and style of the manuscript. We thank Prof. Aimin Xu (The University of Hong Kong) for helpful discussion and critical reading of the revised manuscript.

Funding. This work was supported by National Natural Science Foundation of China (Grant No. 81770771 to S.J.), the Science and Technology Program of Guangzhou China (Grant No. 201704020209 to S.J.) and the National Natural Science Foundation of Guangdong China (Grant No. 2017A030313527 to S.J.).

Conflict of Interest

None

Author Contributions. W.T. designed the study, performed experiments and analyzed the data. Y.Z. and L.M. contributed to the animal experiments, data analysis and figure preparation, and C.D., H.D., X.L. and R.L. contributed to the in vitro experiments. S.L. and T.N. contributed to the figure preparation. W.C. and C.W. contributed to the data analysis. C.B. contributed to study design and edited the manuscript. S.J. supervised the project, analyzed the data and wrote the article. S.J. is the guarantor of this work and takes responsibility for the integrity of the data and the accuracy of the data analysis.

References:

1. Seymour PA, Sander M. Historical perspective: beginnings of the beta-cell: current perspectives in beta-cell development. Diabetes. 2011;60(2):364-76. doi: 10.2337/db10-1068. PubMed PMID: 21270248; PubMed Central PMCID: PMCPMC3028333.
2. Meier JJ, Butler AE, Saisho Y, Monchamp T, Galasso R, Bhushan A, et al. Beta-cell replication is the primary mechanism subserving the postnatal expansion of beta-cell mass in humans. Diabetes. 2008;57(6):1584-94. doi: 10.2337/db07-1369. PubMed PMID: 18334605; PubMed Central PMCID: PMCPMC3697779.
3. Dor Y, Brown J, Martinez OI, Melton DA. Adult pancreatic beta-cell are formed by self-duplication rather than stem-cell differentiation. Nature. 2004;429(6987):41-6. doi: 10.1038/nature02520. PubMed PMID: 15129273.
4. Sachdeva MM, Stoffers DA. Minireview: Meeting the demand for insulin: molecular mechanisms of adaptive postnatal beta-cell mass expansion. Mol Endocrinol. 2009;23(6):747-58. doi: 10.1210/me.2008-0400. PubMed PMID: 19196831; PubMed Central PMCID: PMCPMC2691682.
5. Butler PC, Meier JJ, Butler AE, Bhushan A. The replication of beta-cell in normal physiology, in disease and for therapy. Nat Clin Pract Endocrinol Metab. 2007;3(11):758-68. doi: 10.1038/ncpendmet0647. PubMed PMID: 17955017.
6. Bonner-Weir S. Life and death of the pancreatic beta-cell. Trends Endocrinol Metab. 2000;11(9):375-8. PubMed PMID: 11042468.
7. Dhawan S, Georgia S, Bhushan A. Formation and regeneration of the endocrine pancreas. Curr Opin Cell Biol. 2007;19(6):634-45. doi: 10.1016/j.ceb.2007.09.015. PubMed PMID: 18061427; PubMed Central PMCID: PMCPMC2695413.
8. Gregg BE, Moore PC, Demozay D, Hall BA, Li M, Husain A, et al. Formation of a human beta-cell population within pancreatic islets is set early in life. J Clin Endocrinol Metab. 2012;97(9):3197-206. doi: 10.1210/jc.2012-1206. PubMed PMID: 22745242; PubMed Central PMCID: PMCPMC3431572.
9. Taylor BL, Benthuysen J, Sander M. Postnatal beta-cell proliferation and mass expansion is dependent on the transcription factor Nkx6.1. Diabetes. 2015;64(3):897-903. doi: 10.2337/db14-0684. PubMed PMID: 25277396; PubMed Central PMCID: PMCPMC4338594.
10. Karnik SK, Hughes CM, Gu X, Rozenblatt-Rosen O, McLean GW, Xiong Y, et al. Menin regulates pancreatic islet growth by promoting histone methylation and expression of genes encoding p27Kip1 and p18INK4c. Proc Natl Acad Sci U S A. 2005;102(41):14659-64. doi: 10.1073/pnas.0503484102. PubMed PMID: 16195383; PubMed Central PMCID: PMCPMC1253549.
11. Zhang H, Ackermann AM, Gusarova GA, Lowe D, Feng X, Kopsombut UG, et al. The FoxM1 transcription factor is required to maintain pancreatic beta-cell mass. Mol Endocrinol. 2006;20(8):1853-66. doi: 10.1210/me.2006-0056. PubMed PMID: 16556734.
12. Rane SG, Dubus P, Mettus RV, Galbreath EJ, Boden G, Reddy EP, et al.

Loss of Cdk4 expression causes insulin-deficient diabetes and Cdk4 activation results in beta-islet cell hyperplasia. Nat Genet. 1999;22(1):44-52. doi: 10.1038/8751. PubMed PMID: 10319860.

13. Georgia S, Bhushan A. Beta-cell replication is the primary mechanism for maintaining postnatal beta-cell mass. J Clin Invest. 2004;114(7):963-8. doi: 10.1172/JCI22098. PubMed PMID: 15467835; PubMed Central PMCID: PMCPMC518666.
14. Kushner JA, Ciemerych MA, Sicinska E, Wartschow LM, Teta M, Long SY, et al. Cyclins D2 and D1 are essential for postnatal pancreatic beta-cell growth. Mol Cell Biol. 2005;25(9):3752-62. doi: 10.1128/MCB.25.9.3752-3762.2005. PubMed PMID: 15831479; PubMed Central PMCID: PMCPMC1084308.
15. Krishnamurthy J, Ramsey MR, Ligon KL, Torrice C, Koh A, Bonner-Weir S, et al. p16INK4a induces an age-dependent decline in islet regenerative potential. Nature. 2006;443(7110):453-7. doi: 10.1038/nature05092. PubMed PMID: 16957737.
16. Georgia S, Bhushan A. p27 Regulates the transition of beta-cell from quiescence to proliferation. Diabetes. 2006;55(11):2950-6. doi: 10.2337/db06-0249. PubMed PMID: 17065330.
17. Georgia S, Soliz R, Li M, Zhang P, Bhushan A. p57 and Hes1 coordinate cell cycle exit with self-renewal of pancreatic progenitors. Dev Biol. 2006;298(1):22-31. doi: 10.1016/j.ydbio.2006.05.036. PubMed PMID: 16899237.
18. Fiaschi-Taesch NM, Kleinberger JW, Salim FG, Troxell R, Wills R, Tanwir M, et al. Cytoplasmic-nuclear trafficking of G1/S cell cycle molecules and adult human beta-cell replication: a revised model of human beta-cell G1/S control. Diabetes. 2013;62(7):2460-70. doi: 10.2337/db12-0778. PubMed PMID: 23493571; PubMed Central PMCID: PMCPMC3712040.
19. Gierl MS, Karoulias N, Wende H, Strehle M, Birchmeier C. The zinc-finger factor Insm1 (IA-1) is essential for the development of pancreatic beta-cell and intestinal endocrine cells. Genes Dev. 2006;20(17):2465-78. doi: 10.1101/gad.381806. PubMed PMID: 16951258; PubMed Central PMCID: PMCPMC1560419.
20. Osipovich AB, Long Q, Manduchi E, Gangula R, Hipkens SB, Schneider J, et al. Insm1 promotes endocrine cell differentiation by modulating the expression of a network of genes that includes Neurog3 and Ripply3. Development. 2014;141(15):2939-49. doi: 10.1242/dev.104810. PubMed PMID: 25053427; PubMed Central PMCID: PMCPMC4197673.
21. Jia S, Ivanov A, Blasevic D, Muller T, Purfurst B, Sun W, et al. Insm1 cooperates with Neurod1 and Foxa2 to maintain mature pancreatic beta-cell function. EMBO J. 2015;34(10):1417-33. doi: 10.15252/embj.201490819. PubMed PMID: 25828096; PubMed Central PMCID: PMCPMC4492000.
22. Hija A, Salpeter S, Klochendler A, Grimsby J, Brandeis M, Glaser B, et al. G0-G1 transition and the restriction point in pancreatic beta-cell in vivo. Diabetes. 2014;63(2):578-84. doi: 10.2337/db12-1035. PubMed PMID: 24130333; PubMed Central PMCID: PMCPMC3900543.
23. Darzynkiewicz Z, Gong J, Juan G, Ardelt B, Traganos F. Cytometry of cyclin proteins. Cytometry. 1996;25(1):1-13. doi: 10.1002/(SICI)1097-0320(19960901)25:1<1::AID-CYTO1>3.0.CO;2-N. PubMed PMID:

8875049.
24. Kulkarni RN, Mizrachi EB, Ocana AG, Stewart AF. Human beta-cell proliferation and intracellular signaling: driving in the dark without a road map. Diabetes. 2012;61(9):2205-13. doi: 10.2337/db12-0018. PubMed PMID: 22751699; PubMed Central PMCID: PMCPMC3425429.
25. Whyte WA, Orlando DA, Hnisz D, Abraham BJ, Lin CY, Kagey MH, et al. Master transcription factors and mediator establish super-enhancers at key cell identity genes. Cell. 2013;153(2):307-19. doi: 10.1016/j.cell.2013.03.035. PubMed PMID: 23582322; PubMed Central PMCID: PMCPMC3653129.
26. Pasquali L, Gaulton KJ, Rodriguez-Segui SA, Mularoni L, Miguel-Escalada I, Akerman I, et al. Pancreatic islet enhancer clusters enriched in type 2 diabetes risk-associated variants. Nat Genet. 2014;46(2):136-43. doi: 10.1038/ng.2870. PubMed PMID: 24413736; PubMed Central PMCID: PMCPMC3935450.
27. Schaeffer E, Vigneron M, Sibler AP, Oulad-Abdelghani M, Chatton B, Donzeau M. ATF7 is stabilized during mitosis in a CDK1-dependent manner and contributes to cyclin D1 expression. Cell Cycle. 2015;14(16):2655-66. doi: 10.1080/15384101.2015.1064568. PubMed PMID: 26101806; PubMed Central PMCID: PMCPMC4615120.
28. V EH, Salgado G, Riffo E, Escobar D, Hepp MI, Farkas C, et al. SALL2 represses cyclins D1 and E1 expression and restrains G1/S cell cycle transition and cancer-related phenotypes. Mol Oncol. 2018. doi: 10.1002/1878-0261.12308. PubMed PMID: 29689621.
29. Panda AC, Abdelmohsen K, Martindale JL, Di Germanio C, Yang X, Grammatikakis I, et al. Novel RNA-binding activity of MYF5 enhances Ccnd1/Cyclin D1 mRNA translation during myogenesis. Nucleic Acids Res. 2016;44(5):2393-408. doi: 10.1093/nar/gkw023. PubMed PMID: 26819411; PubMed Central PMCID: PMCPMC4797292.
30. Thorens B, Guillam MT, Beermann F, Burcelin R, Jaquet M. Transgenic reexpression of GLUT1 or GLUT2 in pancreatic beta-cell rescues GLUT2-null mice from early death and restores normal glucose-stimulated insulin secretion. J Biol Chem. 2000;275(31):23751-8. doi: 10.1074/jbc.M002908200. PubMed PMID: 10823833.
31. Orci L, Unger RH, Ravazzola M, Ogawa A, Komiya I, Baetens D, et al. Reduced beta-cell glucose transporter in new onset diabetic BB rats. J Clin Invest. 1990;86(5):1615-22. doi: 10.1172/JCI114883. PubMed PMID: 2243134; PubMed Central PMCID: PMCPMC296911.
32. Thorens B, Weir GC, Leahy JL, Lodish HF, Bonner-Weir S. Reduced expression of the liver/beta-cell glucose transporter isoform in glucose-insensitive pancreatic beta-cell of diabetic rats. Proc Natl Acad Sci U S A. 1990;87(17):6492-6. PubMed PMID: 2204056; PubMed Central PMCID: PMCPMC54562.
33. Mellitzer G, Bonne S, Luco RF, Van De Casteele M, Lenne-Samuel N, Collombat P, et al. IA1 is NGN3-dependent and essential for differentiation of the endocrine pancreas. EMBO J. 2006;25(6):1344-52. doi: 10.1038/sj.emboj.7601011. PubMed PMID: 16511571; PubMed Central PMCID: PMCPMC1422151.
34. Kulkarni RN, Mizrachi EB, Ocana AG, Stewart AF. Human beta-cell proliferation and intracellular signaling: driving in the dark without a road

map. Diabetes. 2012;61(9):2205-13. doi: 10.2337/db12-0018. PubMed PMID: 22751699; PubMed Central PMCID: PMCPMC3425429.
35. Bernal-Mizrachi E, Kulkarni RN, Scott DK, Mauvais-Jarvis F, Stewart AF, Garcia-Ocana A. Human beta-cell proliferation and intracellular signaling part 2: still driving in the dark without a road map. Diabetes. 2014;63(3):819-31. doi: 10.2337/db13-1146. PubMed PMID: 24556859; PubMed Central PMCID: PMCPMC3931400.
36. Zhang T, Liu WD, Saunee NA, Breslin MB, Lan MS. Zinc finger transcription factor INSM1 interrupts cyclin D1 and CDK4 binding and induces cell cycle arrest. J Biol Chem. 2009;284(9):5574-81. doi: 10.1074/jbc.M808843200. PubMed PMID: 19124461; PubMed Central PMCID: PMCPMC2645817.
37. Chen C, Breslin MB, Lan MS. Ectopic expression of a small cell lung cancer transcription factor, INSM1 impairs alveologenesis in lung development. BMC Pulm Med. 2016;16:49. doi: 10.1186/s12890-016-0215-3. PubMed PMID: 27072116; PubMed Central PMCID: PMCPMC4830008.
38. Goto Y, De Silva MG, Toscani A, Prabhakar BS, Notkins AL, Lan MS. A novel human insulinoma-associated cDNA, IA-1, encodes a protein with "zinc-finger" DNA-binding motifs. J Biol Chem. 1992;267(21):15252-7. PubMed PMID: 1634555.
39. Lan MS, Russell EK, Lu J, Johnson BE, Notkins AL. IA-1, a new marker for neuroendocrine differentiation in human lung cancer cell lines. Cancer Res. 1993;53(18):4169-71. PubMed PMID: 8364910.
40. Chen C, Breslin MB, Lan MS. INSM1 increases N-myc stability and oncogenesis via a positive-feedback loop in neuroblastoma. Oncotarget. 2015;6(34):36700-12. doi: 10.18632/oncotarget.5485. PubMed PMID: 26456864; PubMed Central PMCID: PMCPMC4742205.
41. Fujino K, Motooka Y, Hassan WA, Ali Abdalla MO, Sato Y, Kudoh S, et al. Insulinoma-Associated Protein 1 Is a Crucial Regulator of Neuroendocrine Differentiation in Lung Cancer. Am J Pathol. 2015;185(12):3164-77. doi: 10.1016/j.ajpath.2015.08.018. PubMed PMID: 26482608.
42. Kuji S, Watanabe R, Sato Y, Iwata T, Hirashima Y, Takekuma M, et al. A new marker, insulinoma-associated protein 1 (INSM1), for high-grade neuroendocrine carcinoma of the uterine cervix: Analysis of 37 cases. Gynecol Oncol. 2017;144(2):384-90. doi: 10.1016/j.ygyno.2016.11.020. PubMed PMID: 27908529.
43. Li Q, Notkins AL, Lan MS. Molecular characterization of the promoter region of a neuroendocrine tumor marker, IA-1. Biochem Biophys Res Commun. 1997;236(3):776-81. doi: 10.1006/bbrc.1997.7054. PubMed PMID: 9245732.
44. Rosenbaum JN, Guo Z, Baus RM, Werner H, Rehrauer WM, Lloyd RV. INSM1: A Novel Immunohistochemical and Molecular Marker for Neuroendocrine and Neuroepithelial Neoplasms. Am J Clin Pathol. 2015;144(4):579-91. doi: 10.1309/AJCPGZWXXBSNL4VD. PubMed PMID: 26386079.
45. Taniwaki M, Daigo Y, Ishikawa N, Takano A, Tsunoda T, Yasui W, et al. Gene expression profiles of small-cell lung cancers: molecular signatures of lung cancer. Int J Oncol. 2006;29(3):567-75. PubMed PMID: 16865272.
46. Negrini S, Prada I, D'Alessandro R, Meldolesi J. REST: an oncogene or a

tumor suppressor? Trends Cell Biol. 2013;23(6):289-95. doi: 10.1016/j.tcb.2013.01.006. PubMed PMID: 23414932.

47. Naya FJ, Huang HP, Qiu Y, Mutoh H, DeMayo FJ, Leiter AB, et al. Diabetes, defective pancreatic morphogenesis, and abnormal enteroendocrine differentiation in BETA2/neuroD-deficient mice. Genes Dev. 1997;11(18):2323-34. PubMed PMID: 9308961; PubMed Central PMCID: PMCPMC316513.
48. Johnson JD, Ahmed NT, Luciani DS, Han Z, Tran H, Fujita J, et al. Increased islet apoptosis in Pdx1+/- mice. J Clin Invest. 2003;111(8):1147-60. doi: 10.1172/JCI16537. PubMed PMID: 12697734; PubMed Central PMCID: PMCPMC152933.
49. Liu WD, Wang HW, Muguira M, Breslin MB, Lan MS. INSM1 functions as a transcriptional repressor of the neuroD/beta2 gene through the recruitment of cyclin D1 and histone deacetylases. Biochem J. 2006;397(1):169-77. doi: 10.1042/BJ20051669. PubMed PMID: 16569215; PubMed Central PMCID: PMCPMC1479746.

Figure legends

Figure 1. Decreased Insm1 level in *Insm1*$^{+/lacZ}$ mice results in low beta-cell mass and impaired blood glucose levels

(A) Western blot analysis of Insm1 and Pdx1 protein levels in pancreatic islets of 2-month-old wild-type and *Insm1*$^{+/lacZ}$ mice (left). Quantification of the Western blot (right). n=4 for each genotype. (B) Fasted and randomly fed blood glucose levels of 2-month-old wild-type and *Insm1*$^{+/lacZ}$ mice (n=8 for each genotype). (C) Glucose tolerance test of 2-month-old wild-type and *Insm1*$^{+/lacZ}$ mice. The area under the curves are 342.88±92.54 mg.h/dl and 458.53±90.74 mg.h/dl for wild-type and *Insm1*$^{+/lacZ}$ mice, respectively, with an increase of 115.65 mg.h/dl in *Insm1*$^{+/lacZ}$ mice compared to wild-type animals (n=11 for *Insm1*$^{+/+}$ and n=10 for *Insm1*$^{+/lacZ}$; two-tailed unpaired Student's t-test, P=0.012). (D) Glucose-stimulated insulin secretion of 2-month-old wild-type and *Insm1*$^{+/lacZ}$ mice (n=8 for each genotype). (E) Fasted and randomly fed blood glucagon levels of 2-month-old wild-type and *Insm1*$^{+/lacZ}$ mice (n=5 for each genotype). (F) Insulin tolerance test of 2-month-old wild-type and *Insm1*$^{+/lacZ}$ mice (n=6 for each genotype). (G) Insulin secretion response to low (3.3 mM) and high (16.7 mM) glucose in isolated 2-month-old wild-type and *Insm1*$^{+/lacZ}$ islets (n=4 for each genotype). (H) Pancreatic beta-cell mass analyzed in 2-day, 7-day, 14-day, 2-month and 13-month-old wild-type and *Insm1*$^{+/lacZ}$ mice (n=6 for each genotype at each stage). Data are presented as the mean ± SD; statistical significance was assessed by a two-tailed unpaired Student's t-test. ns: P>0.05, *P < 0.05, **P< 0.01, ***P<0.001.

Figure 2. Prolonged cell cycle in pancreatic beta cells of *Insm1*$^{+/lacZ}$ mice

(A) TUNEL analysis indicates apoptosis in pancreatic beta cells at postnatal days 2, 7 and 14 in wild-type and *Insm1*$^{+/lacZ}$ mice (n=5 animals per genotype per stage, 4000 insulin+ cells per animal were counted). (B) Ki67 proliferation analysis in pancreatic beta cells at postnatal days 2, 7 and 14 in wild-type and *Insm1*$^{+/lacZ}$ mice (n=5 per genotype per stage). (C) Illustration of the experimental strategy and the delayed cell cycle detected by BrdU and Ki67 double labeling. BrdU was injected once, followed by a 23 h chase. The BrdU^{+}Ki67^{-} cells have finished the cell cycle during the 23 h chase period, and

the $BrdU^+Ki67^+$ cells indicate cells still in the cell cycle. The average cell cycle time for beta cells is approximately 23 h. The difference in the number of $BrdU^+Ki67^-$ and $BrdU^+Ki67^+$ in wild-type and *Insm1*$^{+/lacZ}$ beta cells indicates a difference in the relative time needed to finish one cycle of cell division. (D) Immunostaining of insulin, Ki67 and BrdU in the pancreas of wild-type and *Insm1*$^{+/lacZ}$ mice at P14. Red arrows indicate $BrdU^+Ki67^-$ beta cells (E). Quantification of the immunostaining showed in (D) for $BrdU^+Ki67^-$ and $BrdU^+Ki67^+$ beta-cell (600 $BrdU^+$ cells were counted from 4-6 sections per animal, 5 animals per genotype). Data are presented as the mean ± SD; statistical significance was assessed by a two-tailed unpaired Student's t-test. *P < 0.05.

Figure 3. Ccnd1 is downregulated in islets of *Insm1*$^{+/lacZ}$ mice and Ccnd1 levels regulate cell cycle length

(A) PI staining and flow cytometry analysis of cell cycle (n=4, two-tailed unpaired Student's t-test compared to siCon: P=0.033 (si*Insm1*), P=0.012 (si*Ccnd1*), P=0.13 (si*Insm1*+*Ccnd1* plasmid)). (B) Expression of cell cycle genes in islets of 14-day-old wild-type and *Insm1*$^{+/lacZ}$ mice (n=5 for each genotype). (C) Ccnd1 protein levels in islets isolated from 14-day-old wild-type and *Insm1*$^{+/lacZ}$ mice (n=4). (D) Analysis of cell cycle length by BrdU and Ki67 double labeling in control, knockdown of *Insm1*, *Ccnd1* and *Insm1* knockdown combined with overexpression of *Ccnd1* in SJb cells (n=4). (B, C, D) Data are presented as the mean ± SD; statistical significance was assessed by a two-tailed unpaired Student's t-test. *P < 0.05.

Figure 4. *Glut2* expression is downregulated in islets of *Insm1*$^{+/lacZ}$ mice

(A) Expression of metabolic genes and transcription factors in islets of 14-day-old wild-type and *Insm1*$^{+/lacZ}$ mice (n=5 for each genotype). (B) Glut2 and Neurod1 protein levels in islets isolated from 14-day-old wild-type and *Insm1*$^{+/lacZ}$ mice. Left, representative blot; right, quantifications (n=4 for each genotype). Data are presented as the mean ± SD; statistical significance was assessed by a two-tailed unpaired Student's t-test. *P < 0.05, **P < 0.01.

Figure 5. Dosage effects and binding affinities of Insm1

(A) ChIP-seq traces of Insm1 binding sites and the reads on *Ccnd1, Pdx1, Hk1* and *Slc2a2 (Glut2)* loci in SJb cells. (B, left) Insm1 protein levels in control and *Insm1* siRNA transfected SJb cells detected by Western blot. Top panel shows the representative blot, bottom panel indicates the quantification (n=4). (B, right) ChIP using an Insm1 antibody in control and Insm1 knockdown SJb cells, qPCR showing the relative amount of Insm1 binding to the indicated loci in control and *Insm1* siRNA transfected cells. Fold change of binding (sicon vs siInsm1) on the individual gene loci: *Ccnd1-pro* 8.8, *Ccnd1_intron* 10.3, *Pdx1* 1.7, *Hk1* 1.4, *Glut2* 5.7, *Gapdh* 0.5 (n=4). (C) ChIP-PCR from islets of 14-day-old wild-type and *Insm1*$^{+/lacZ}$ mice (n=4). Data are presented as the mean ± SD. Two-tailed unpaired Student's t-test, ns: P>0.05, *P < 0.05, **P<0.01, ***P<0.001

Figure 6. The ratio of beta-cell mass between wild-type and *Insm1*$^{+/lacZ}$ mice is maintained during metabolic stress

(A,B,C) Glucose tolerance test in wild-type and *Insm1*$^{+/lacZ}$ mice on an *ob/ob* background (A), treated with normal chow (NC) (B) or a high-fat diet (HFD) (C). The area under the curves for wild-type and *Insm1*$^{+/lacZ}$ mice are 367.82±148.12 mg.h/dl and 595.48±86.44 mg.h/dl (n=8, two-tailed unpaired Student's t-test, P=0.0035) (A), 208.63±52.65 mg.h/dl and 346.47±14.16 mg.h/dl (n=6, two-tailed unpaired Student's t-test, P=0.0076) (B), 309.14±62.81 mg.h/dl and 675.28±155.91 mg.h/dl (n=8, two-tailed unpaired Student's t-test, P= 0.000055) (C), respectively, with the enlargement of 227.66 mg.h/dl (A), 137.84 mg.h/dl (B) and 366.15 mg.h/dl (C) in *Insm1*$^{+/lacZ}$ mice (0.5 g/kg glucose per bodyweight was used for *ob/ob* mice and 2 g/kg used for NC and HFD mice). Blood glucose tests from fasted (D) and randomly fed (E) wild-type and *Insm1*$^{+/lacZ}$ mice on a HFD or *ob/ob* background (n=8 for *Insm1*$^{+/+}$ and n=12 for *Insm1*$^{+/lacZ}$). (F) Analysis of beta-cell mass in wild-type and *Insm1*$^{+/lacZ}$ animals on a HFD or *ob/ob* background (n=6). (G) Relative gene expression in 13-month-old wild-type and *Insm1*$^{+/lacZ}$ mice (n=3). (H) ChIP-PCR from islets of 13-month-old *Insm1*$^{+/+}$ and *Insm1*$^{+/lacZ}$ mice (n=4). Data are presented as the mean ± SD; statistical significance was assessed by a two-tailed unpaired Student's t-test. ns: P>0.05, *P < 0.05, **P < 0.01, ***P<0.001.

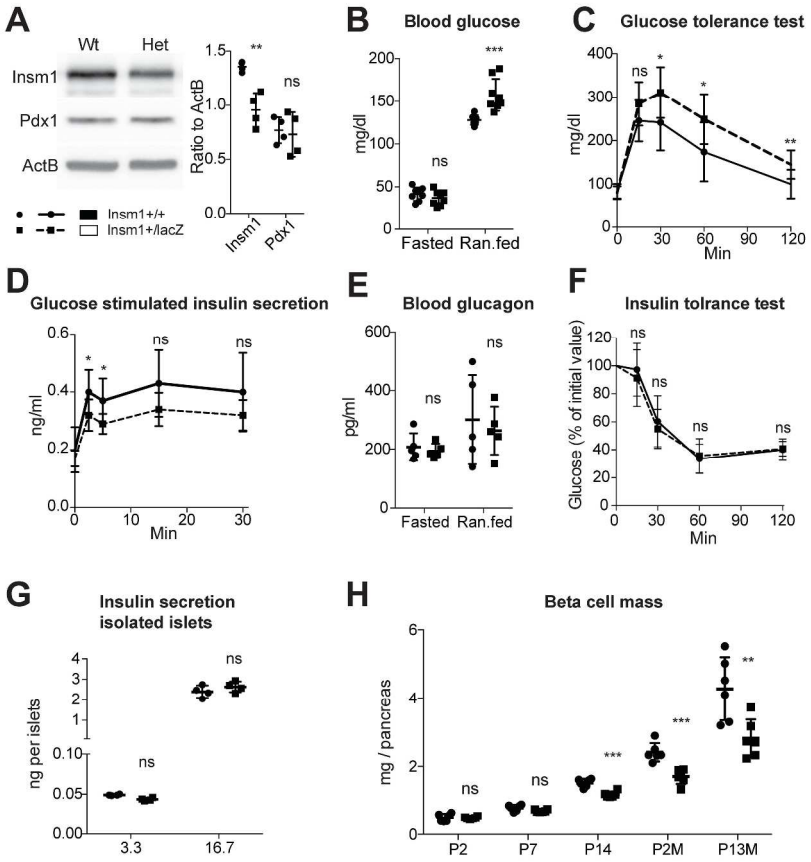

Figure 1. Decreased Insm1 level in Insm1+/lacZ mice results in low beta-cell mass and impaired blood glucose levels

297x420mm (300 x 300 DPI)

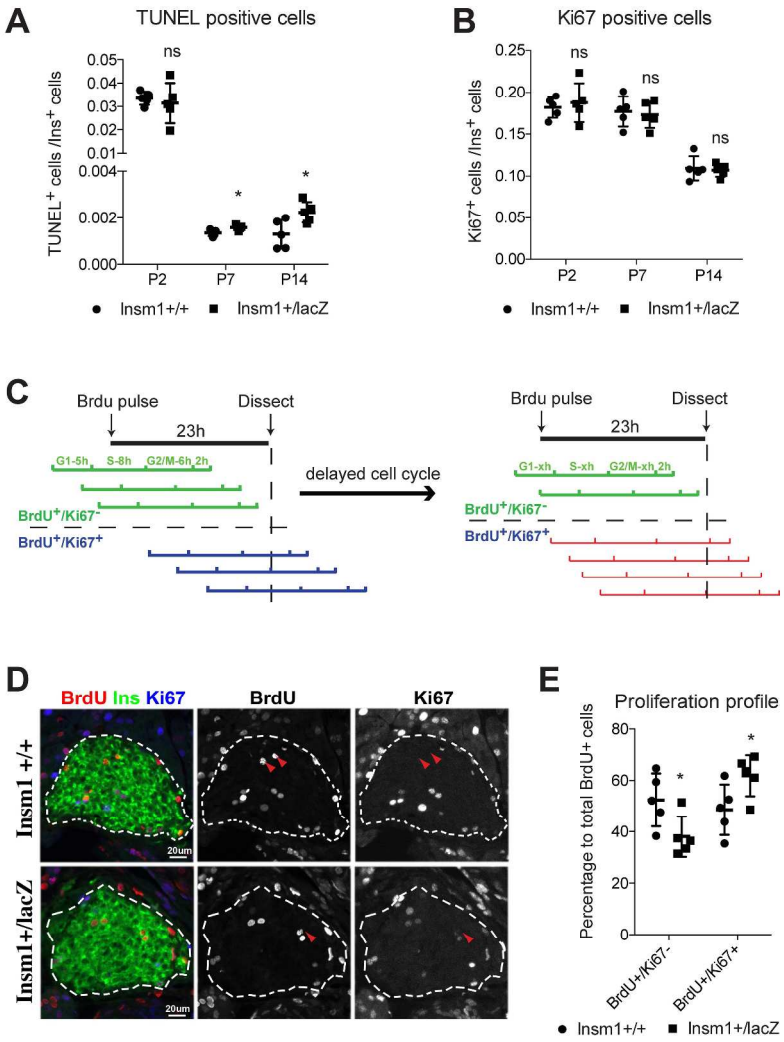

Figure 2. Prolonged cell cycle time in pancreatic beta-cell of Insm1+/lacZ mice

297x420mm (300 x 300 DPI)

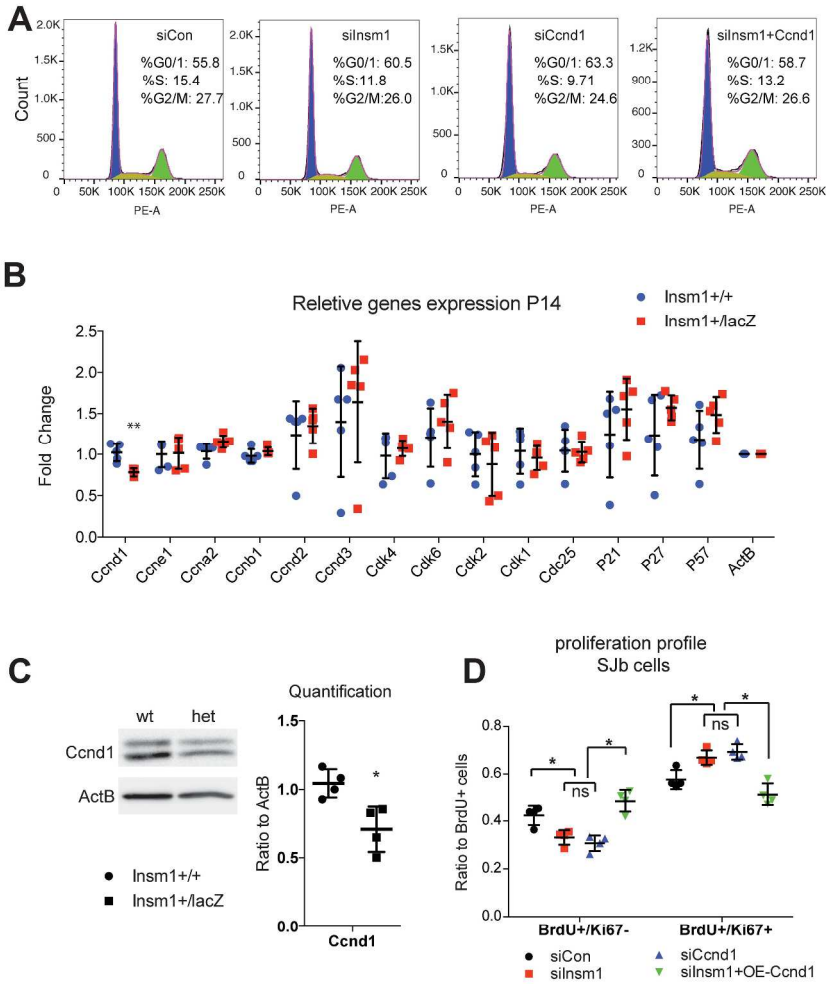

Figure 3. Ccnd1 is downregulated in islets of Insm1+/lacZ mice and Ccnd1 expression levels regulate cell cycle length

297x420mm (300 x 300 DPI)

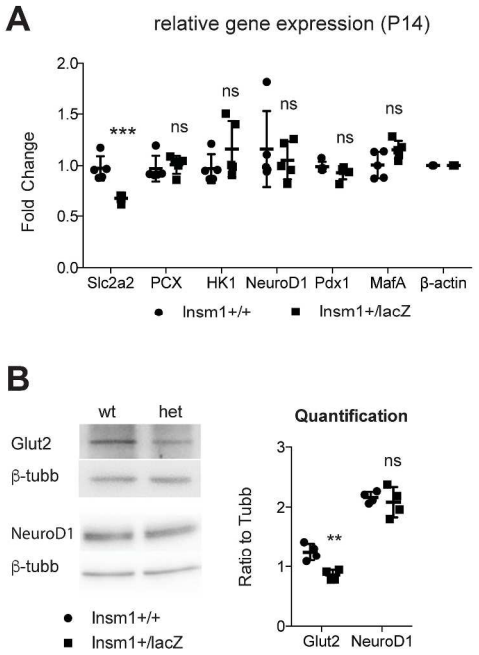

Figure 4. Glut2 expression is downregulated in islets of Insm1+/lacZ mice

297x420mm (300 x 300 DPI)

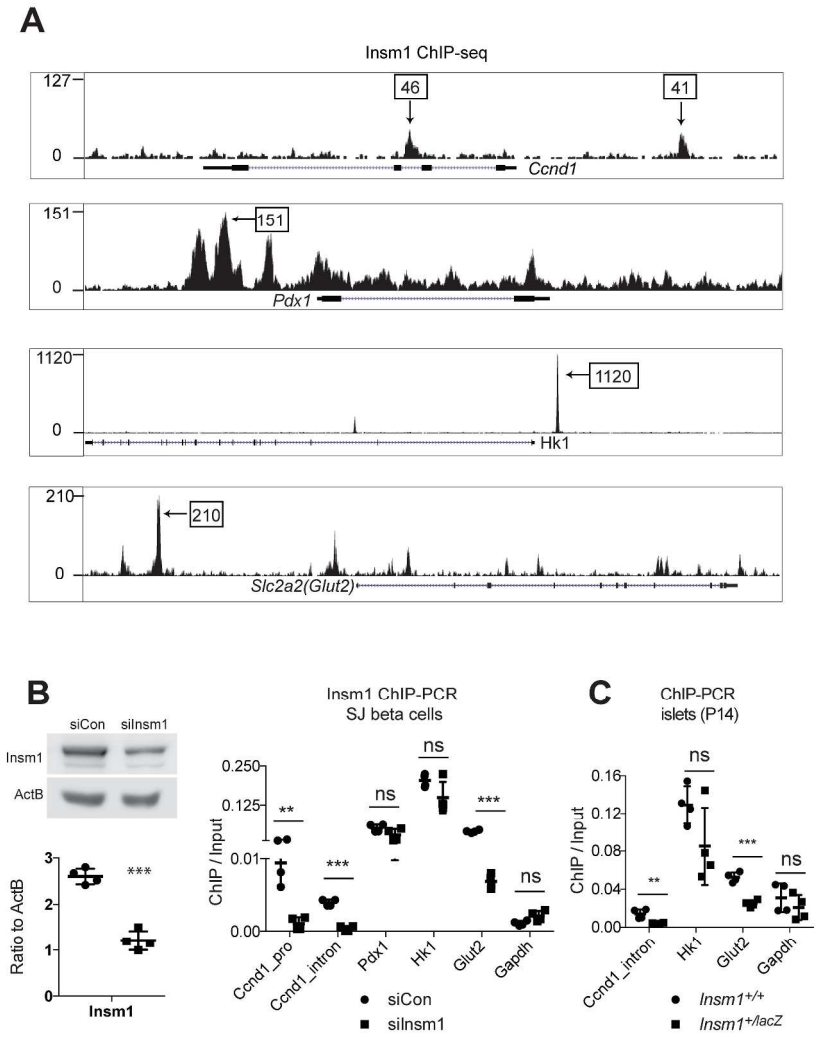

Figure 5. Dosage effects and binding affinities of Insm1

297x420mm (300 x 300 DPI)

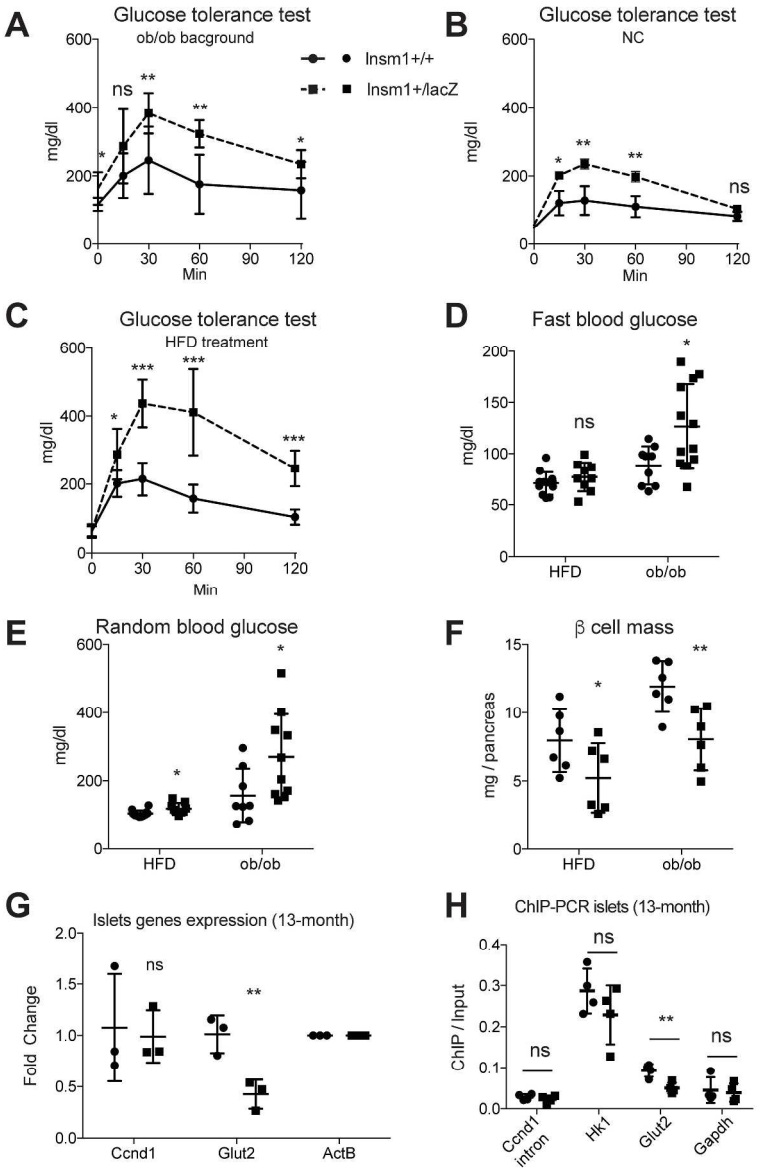

Figure 6. The ratio of beta-cell mass between wild-type and Insm1+/lacZ mice is maintained during metabolic stress

297x420mm (300 x 300 DPI)

Supplimental table . Primes used in relative gene expression and ChIP-PCR

q-PCR primers

ccnd1_RT_fw	GCATGTTCGTGGCCTCTAAG
ccnd1_RT_rv	GTTCCACTTGAGCTTGTTCACC
ccne1_RT_fw	AGGTGTGCGAAGTCTATAAGCTC
ccne1_RT_rv	AGCGCCATCTGTAACATAAGCAA
ccnb1_RT_fw	TAATCCTTGCAGTGAGTGACG
ccnb1_RT_rv	CATCTGAACCTGTATTAGCCAGT
ccna2_RT_fw	TCTTAGAAGACAAGCCAGTGAAC
ccna2_RT_rv	CTGCCTCTTCATGTAACCCAC
mCcnd2_RT_fw	ACCTCCCGCAGTGTTCCTATT
mCcnd2_RT_rv	ACTCCAGCCAAGAAACGGTC
mCcnd3_RT_fw	CTGCTCTATGTCTGCGGATGA
mCcnd3_RT_rv	TGTGGGAGTGCTGGTCTGA
mCdk4_RT_fw	AGCGTAAGATCCCCTGCTTC
mCdk4_RT_rv	AGCACAGACATCCATCAGCC
mCdk6_RT_fw	CCTTACCTCGGTGGTCGTC
mCdk6_RT_rv	TCCTGGGAGTCCAATGATGTC
mCdk2_RT_fw	TCCCCTGGATGAAGATGGAC
mCdk2_RT_rv	CAAGTCAGACCACGGGTGAA
mCdk1_RT_fw	TTGCCAGAGCGTTTGGAATAC
mCdk1_RT_rv	ATCTCTGAGTCGCCGTGGA
mP21_RT_fw	GCCTTGTCGCTGTCTTGC
mP21_RT_rv	GGGCACTTCAGGGTTTTCTC
mP27_RT_fw	TTGGGTCTCAGGCAAACTCT
mP27_RT_rv	GGGGAACCGTCTGAAACATT
mP57_RT_fw	GGGTGTCCCTCTCCAAACG
mP57_RT_rv	CGAAAGGTCCCAGCCGAAG
mCdc25_RT_fw	ACCCAATGGAGTGTTCCCTG
mCdc25_RT_rv	GGCAGCACACACACCTTTGA
mP16_RT_fw	TTTGTGTACCGCTGGGAACG
mP16_RT_rv	GCTCTGCTCTTGGGATTGGC
mSlc2a2_RT_fw	CATTGGCACATCCTACTTGG
mSlc2a2_RT_rv	ACGGAGACCTTCTGCTCAGT
mPcx_RT_fw	GCTGACCCTAGTCGCACTAA
mPcx_RT_rv	CACACCTGCCCCTGATGTAT
mHk1_RT_fw	AACAGCAGAGCTACGGTCAAA
mHk1_RT_rv	TTCCCACTACGGATCTTTACC
mNeurod1_RT_fw	CTCCAGGGTTATGAGATCGTC
mNeurod1_RT_rv	GCTCTCGCTGTATGATTTGGTC
mPdx1_RT_fw	CTCCCTTTCCCGTGGATGAA
mPdx1_RT_rv	GGTCCCGCTACTACGTTTCT
mMafA_RT_fw	GCCACCACGTGCGCTTG
mMafA_RT_rv	CCGCTTCTGTTTCAGTCGGAT

mActB_RT_fw	AGCAGTTGGTTGGAGCAAACATCC
mActB_RT_rv	ACAGAAGCAATGCTGTCACCTTCC

ChIP-PCR primers

Ccnd1_ChIP_profw	GCCGCGCTTACCGTAAACCT
Ccnd1_ChIP_prorv	TGAAGCGCAGGCTCAACCAC
Ccnd1_ChIP_intrF2	ACACCGCCCACATTTCAGAG
Ccnd1_ChIP_intrR2	CAGTGAGCAGAATGCCAACCC
Pdx1_ChIP_fw	GGAAGCCAATTTACCAAAATGC
Pdx1_ChIP_rv	GGTTATGAGCGAGACTTGGG
HK1_ChIP_fw	TGCCCGGAAGATGATACAGAC
HK1_ChIP_rv	AGGCTGTTATCGGGAGAAATGA
Slc2a2_ChIP_fw	AAGCCACTGAGTTGTTGGGAAT
Slc2a2_ChIP_rv	GACACAGCTCCAGACCCGAT
mGapdh_ChIP_fw	AGCCCTTGAGCCTTATTGTCC
mGapdh_ChIP_rv	GACCTCTGTAAGTCCGCTTT

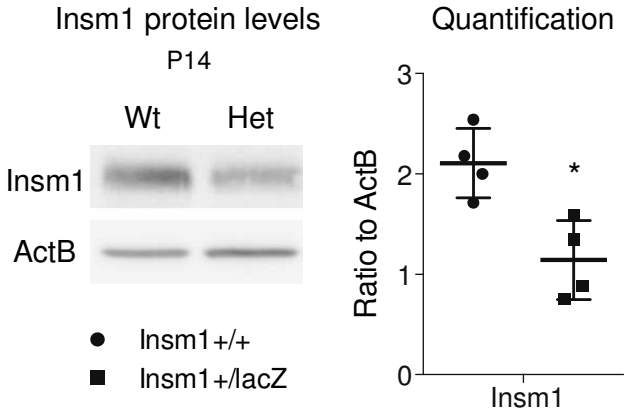
Insm1 protein levels
P14
Wt
Het
Insm1
ActB
Insm1+/+
Insm1+/lacZ
Quantification
Ratio to ActB
3
2
1
0
*
Insm1

Fig. S1

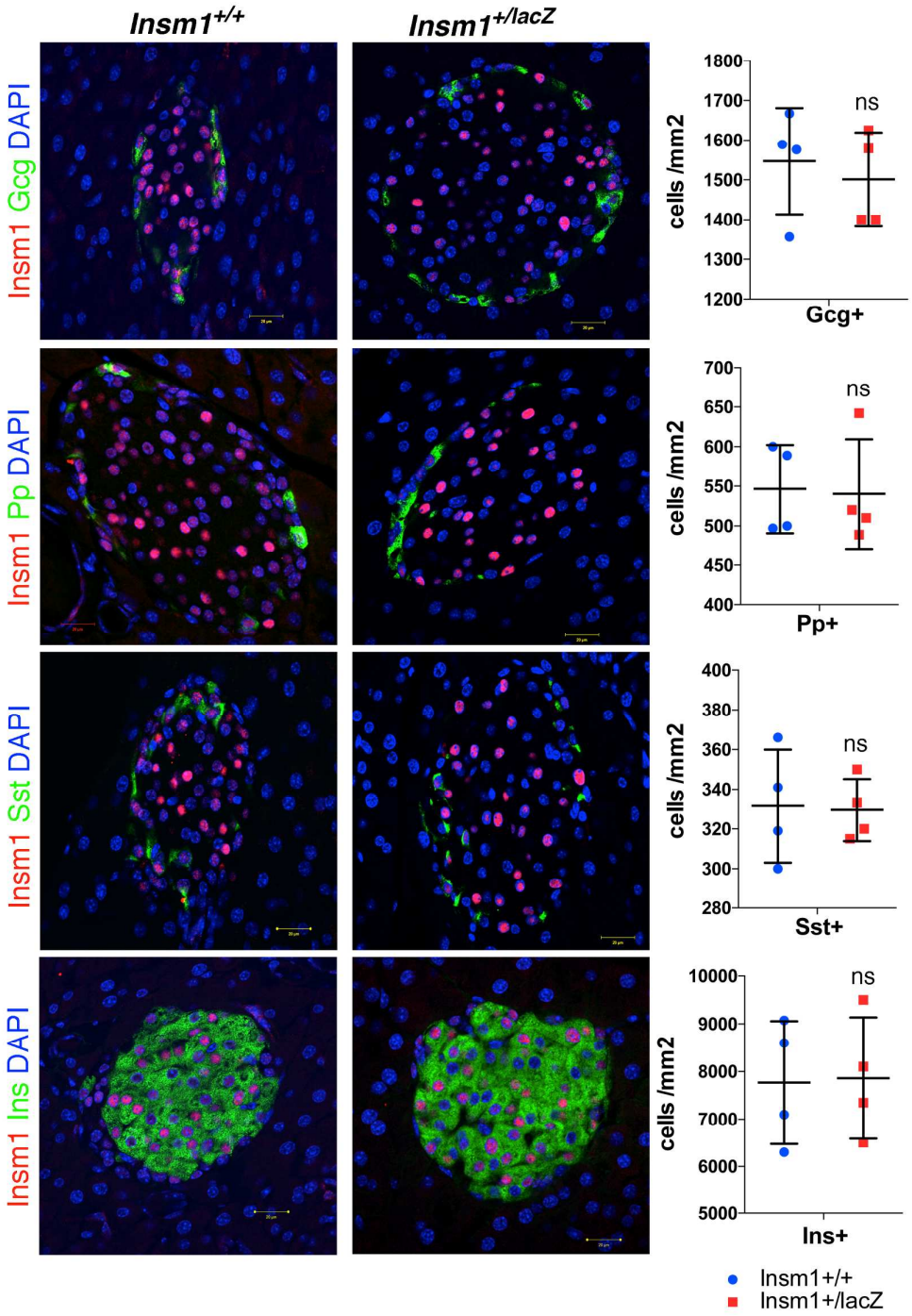
Insm1+/+
Insm1+/lacZ
Insm1 Gcg DAPI
Insm1 Pp DAPI
Insm1 Sst DAPI
Insm1 Ins DAPI
cells /mm2
ns
Gcg+
Pp+
Sst+
Ins+
Insm1+/+
Insm1+/lacZ

Fig. S2

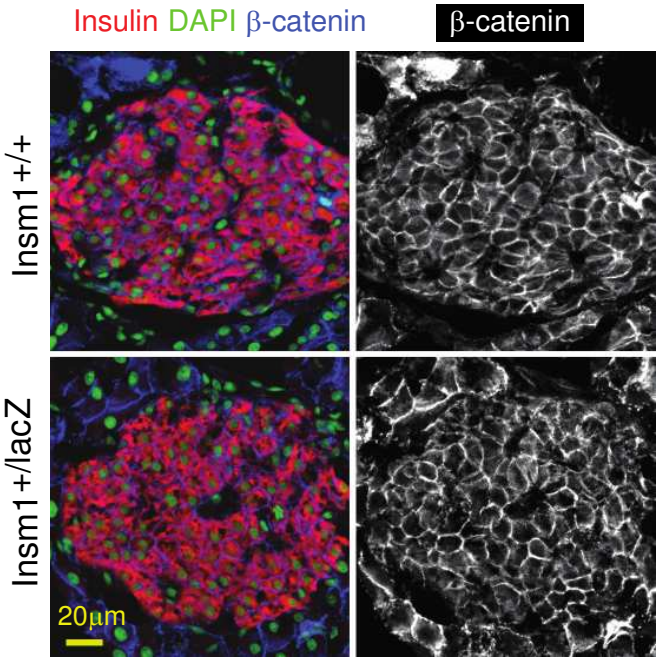
Insulin DAPI β-catenin
β-catenin
Insm1+/+
Insm1+/lacZ
20μm

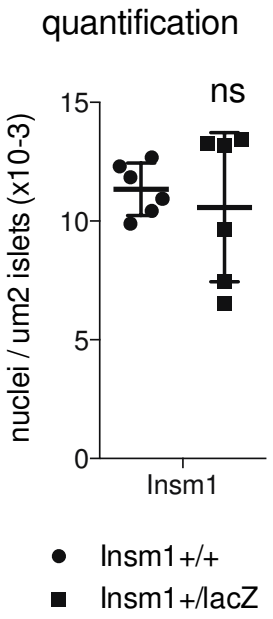
quantification
ns
nuclei / um2 islets (x10-3)
15
10
5
0
Insm1
Insm1+/+
Insm1+/lacZ

Fig S3

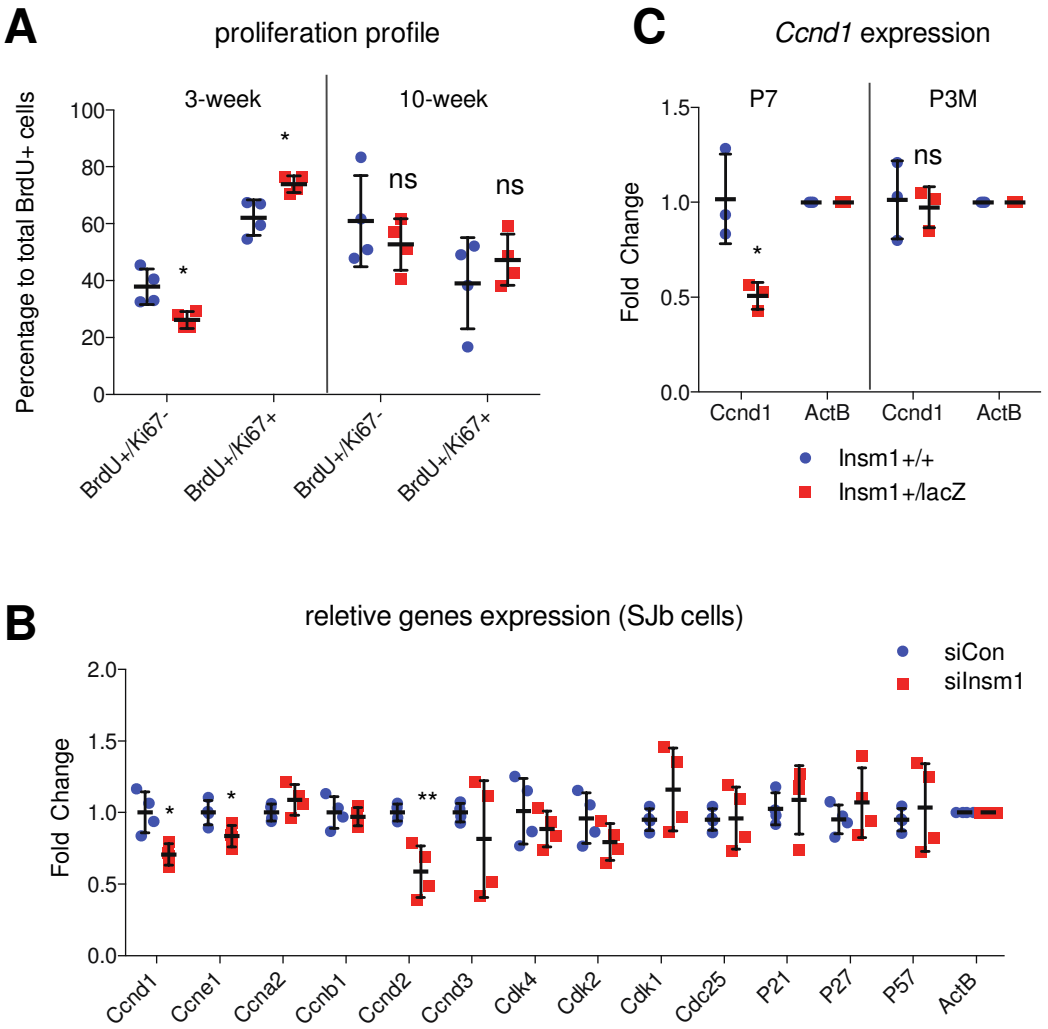
A
proliferation profile
3-week
10-week
Percentage to total BrdU+ cells
100
80
60
40
20
0
*
*
ns
ns
BrdU+/Ki67-
BrdU+/Ki67+
BrdU+/Ki67-
BrdU+/Ki67+
C
Ccnd1 expression
P7
P3M
Fold Change
1.5
1.0
0.5
0.0
*
ns
Ccnd1
ActB
Ccnd1
ActB
Insm1+/+
Insm1+/lacZ
B
reletive genes expression (SJb cells)
siCon
siInsm1
Fold Change
2.0
1.5
1.0
0.5
0.0
*
*
**
Ccnd1
Ccne1
Cna2
Ccnb1
Ccnd2
Ccnd3
Cdk4
Cdk2
Cdk1
Cdc25
P21
P27
P57
ActB

Fig. S4

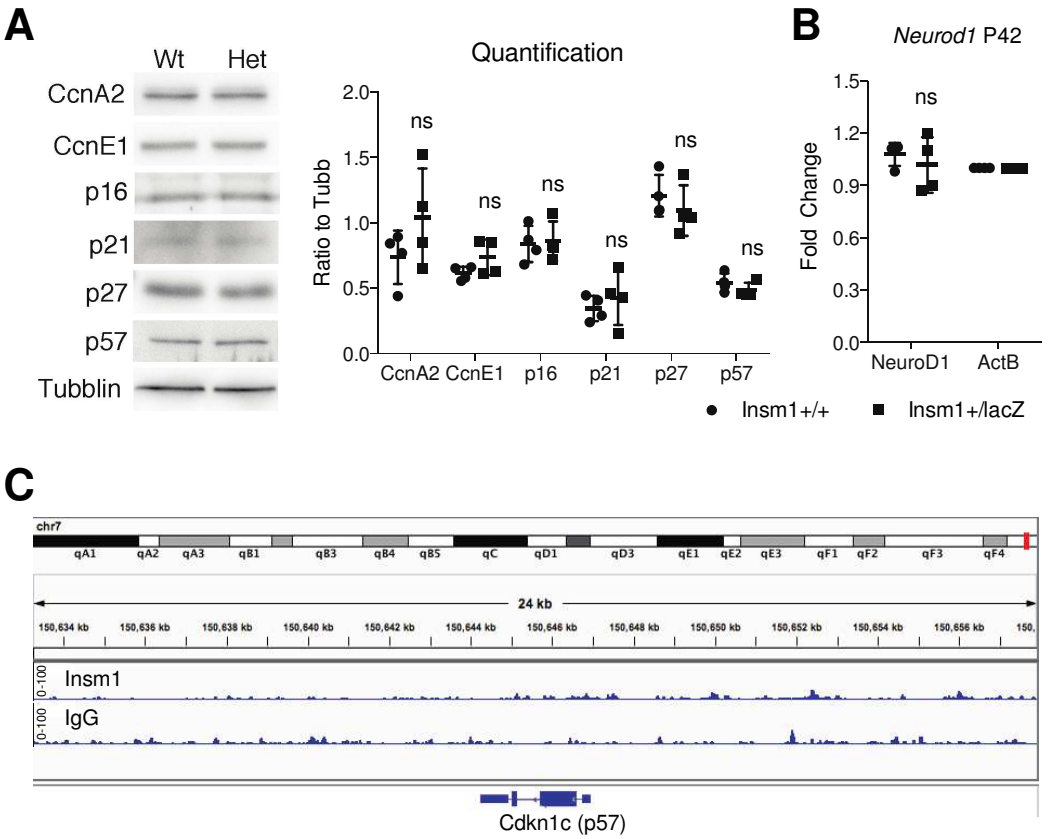
A
Wt
Het
CcnA2
CcnE1
p16
p21
p27
p57
Tubblin
Quantification
Ratio to Tubb
2.0
1.5
1.0
0.5
0.0
ns
CcnA2 CcnE1 p16 p21 p27 p57
B
Neurod1 P42
Fold Change
1.5
1.2
0.9
0.6
0.3
0.0
NeuroD1 ActB
Insm1+/+
Insm1+/lacZ
C
chr7
24 kb
Insm1
IgG
0-100
Cdkn1c (p57)

Fig S5

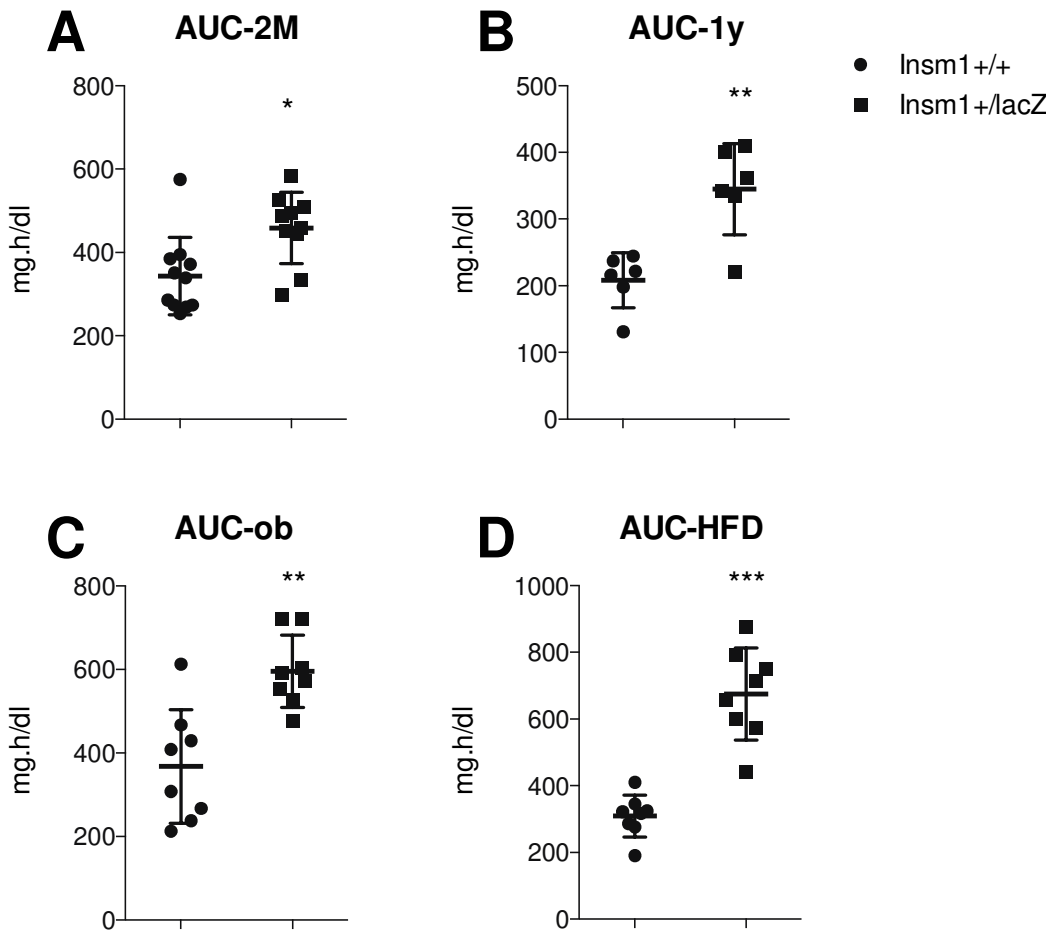

Fig S6

Figure S1. Insm1 expression levels in islets of *Insm1*$^{+/lacZ}$ mice

Insm1 expression levels in P14 islets of *Insm1*$^{+/+}$ and *Insm1*$^{+/lacZ}$ mice detected by Western blot (left); Quantification of the expression levels (right, n=4). Data are presented as means ± SD. Statistical significance was assessed by 2-tailed unpaired Student's t-test. *: P<0.05

Figure S2. Proportions of endocrine cells in in islets of *Insm1*$^{+/lacZ}$ mice

Immunostaining of Insm1, DAPI and endocrine cell markers Gcg / Pp / Sst / Ins in islets of 2-month old *Insm1*$^{+/+}$ and *Insm1*$^{+/lacZ}$ mice (left). Quantification

of the islets endocrine cell types, 400 cells for Gcg/Pp/Sst positive cells and 2000 cells for Ins positive cells were counted. (Animal number n=4 for each genotype). Data are presented as means ± SD. Statistical significance was assessed by 2-tailed unpaired Student's t-test. ns: P>0.05.

Figure S3. Pancreatic beta cell size of *Insm1*$^{+/+}$ and *Insm1*$^{+/lacZ}$ mice

Staining of Insulin, beta-catenin and DAPI in pancreas of *Insm1*$^{+/+}$ and *Insm1*$^{+/lacZ}$ mice at the age of 2-month (left), quantification of beta cell size by measuring insulin positive area and counting of DAPI number in Insulin positive cells (right). (Counting 2000 cell per animal, Animal number n=6). Data are presented as means ± SD. Statistical significance was assessed by 2-tailed unpaired Student's t-test. ns: P>0.05.

Figure S4. Cell cycle length and *Ccnd1* expression in islets of *Insm1*$^{+/lacZ}$ mice

(A) Quantification of BrdU^{+}Ki67^{-} and BrdU^{+}Ki67^{+} beta cells (600 BrdU^{+} cells per animal and 4 animals per genotypes) in islets of *Insm1*$^{+/+}$ and *Insm1*$^{+/lacZ}$ mice at the ages of 3-week and 10-week. (B) Expression of cell cycle genes in non-target siRNA and *Insm1* specific siRNA treated SJb cells (n=4 for each cell treatment). (C) The mRNA levels of *Ccnd1* in islets of postnatal 7-day and 3-month old animals (animal number n=3 for each genotype). Data are presented as means ± SD. Statistical significance was assessed by 2-tailed unpaired Student's t-test, *: P < 0.05.

Figure S5. Indicated genes expression under Insm1-dosage deficiency

(A) Protein levels of CcnE1, CcnA2, p16, p21, p27 and p57 in P14 islets of *Insm1*$^{+/+}$ and *Insm1*$^{+/lacZ}$ mice (n=4). (B) *NeuroD1* mRNA level in P42 islets detected by qRT-PCR (n=4). (C) No Insm1 binding on Cdkn1c locus. Up trace, Insm1 ChIP-seq; low trace, IgG ChIP-seq trace. IgG ChIP-seq trace was used as non-binding control. Data are presented as means ± SD. Statistical significance was assessed by 2-tailed unpaired Student's t-test, ns: P>0.05.

Figure S6. The area under the curves (AUCs) analysis of GTT related to Fig.1 and Fig. 6

(A) AUC of GTT on 2-month old Insm1$^{+/+}$ and Insm1$^{+/lacZ}$ mice (n=11 for Insm1$^{+/+}$ and n=10 for Insm1$^{+/lacZ}$). (B) AUC of GTT on 1-year old Insm1$^{+/+}$ and Insm1$^{+/lacZ}$ mice treated with NC (n=6). (C) AUC of GTT on an ob/ob background Insm1$^{+/+}$ and Insm1$^{+/lacZ}$ mice (n=8). (D) AUC of GTT on Insm1$^{+/+}$ and Insm1$^{+/lacZ}$ mice treated with HFD (n=8). Two-tailed unpaired Student's t-test, *P < 0.05, **P<0.01, ***P<0.001.